Direct Measurement of Chain Order in Single Phospholipid Mono- and Bilayers with Multiplex CARS

George W. H. Wurpel, Juleon M. Schins,† and Michiel Müller*

Swammerdam Institute for Life Sciences, University of Amsterdam, P.O. Box 94062, 1090 GB Amsterdam, The Netherlands

Received: November 27, 2003; In Final Form: January 16, 2004

We present direct measurements of the thermodynamic state of single phospholipid mono- and bilayers based on the intrinsic vibrational properties of the molecules. The increased, shot-noise limited, sensitivity of multiplex coherent anti-Stokes Raman scattering permits the acquisition of vibrational spectra of single lipid bilayers with a signal-to-noise ratio of 4 in 20 ms. The lipid chain order for both liquid-crystalline and gel phase supported lipid bilayers is determined. Using deuterated lipids, vibrational spectra can be measured selectively in either of the leaflets of an asymmetric bilayer.

Coherent anti-Stokes Raman scattering (CARS) microscopy is becoming an increasingly popular method to obtain molecular information at high spatial resolution,[1,2] owing to its unique capability to visualize both chemical composition and structural features in a variety of specimens by their vibrational spectra, i.e., without the use of labels. With this technique, spectral parameters, e.g., line widths, resonance frequencies, and amplitudes, can be obtained for every position in the sample. This is accomplished most conveniently in a multiplex CARS setup, where a significant part of the vibrational spectrum is measured simultaneously. Using a multiplex CARS microscope, we have recently demonstrated vibrational mapping of chemical and physical structures in lipid multilamellar vesicles (MLV).[3,4] However, MLVs represent dense lipid structures. To be relevant for lipid studies in biomimetic and biological systems, the sensitivity of CARS microscopy should allow the imaging of chemical components within, or physical structure of, a single lipid bilayer. Here, this is accomplished for the first time with the measurement of vibrational spectra of single phospholipid mono- and bilayers with a signal-to-noise ratio (SNR) of 4 in 20 ms.[5] Because the signal strength falls off linearly with concentration and the SNR of the multiplex CARS spectrum is limited only by shot-noise, the accuracy and sensitivity of the measurement can be increased through a proportional increase of the spectral acquisition time.

Owing to the increased sensitivity of this heterodyne technique, we could measure and distinguish vibrational spectra of planar supported bilayers of saturated and unsaturated phospholipids on a glass−water interface, which are in the gel and liquid crystalline phase respectively at room temperature. The ability to directly detect the thermodynamic phase of a membrane is relevant to cell biology, where phase domains, so-called lipid rafts, are thought to play an important role in a number of cellular functions.[6] The structural changes that accompany a transition from gel to liquid crystalline phase, such as changes in packing and acyl chain order, cause significant changes in the C−H stretch vibrations. Based on these vibrational fingerprints, we determine a lipid chain order parameter of single lipid bilayers from a multiplex CARS spectral analysis. Furthermore, we show that we can also address asymmetric bilayers, using deuterated lipids to selectively image one leaflet of the membrane.

CARS is a four-wave parametric mixing process, where a pump (ω_p) and a Stokes (ω_S) laser field generate an anti-Stokes signal at $\omega_{CARS} = 2\omega_p - \omega_S$ in the phase-matching direction. Resonant enhancement occurs when the energy difference $\omega_p - \omega_S$ equals that of a vibrational transition. In multiplex CARS, different resonance conditions may be simultaneously fulfilled over the large spectral bandwidth of ω_S. As the spectral resolution is determined by ω_p, this allows for the collection of CARS spectra over a wide frequency range without the necessity of wavelength tuning. Thus, in a single shot, the whole C−H stretch (2800−3100 cm^{-1}) or C−D stretch region (2000−2300 cm^{-1}) of the vibrational spectrum can be captured. An energy level diagram of the multiplex CARS process is depicted in Figure 1a.

The signal that is generated in CARS is generally orders of magnitude larger than that of spontaneous Raman scattering and is not obscured by a luminescent background. This improved signal level, however, does not directly lead to a higher SNR, because the CARS four-photon interaction always produces a nonresonant background signal. In single-frequency CARS, variations in this background intensity due to laser-related fluctuations, easily obscure weak Raman signals. It is possible to suppress the nonresonant signal through a polarization scheme,[7,8] epi-detection,[9] time-resolved measurements,[10] or combined phase and polarization control,[11] but these background free methods also reduce the total signal yields. Alternatively, high sensitivity in CARS can be obtained, as shown in this paper, by *using* rather than *suppressing* the nonresonant background to maximize the total signal yield. A multiplex approach is essential here to obtain shot-noise limited detection sensitivity. The same heterodyne technique has been applied in sum-frequency generation spectroscopy[12,13] and, in a somewhat different context, in single-pulse CARS spectroscopy.[14]

To illustrate this approach, consider the following: far away from one-photon resonances, the CARS signal for a dilute solute

* To whom correspondence should be addressed. E-mail: muller@science.uva.nl.

† Current address: Radiation Chemistry Department, Interfaculty Reactor Institute, Delft University of Technology Mekelweg 15, 2629 JB Delft, The Netherlands.

10.1021/jp037629j CCC: $27.50
Published on Web 02/24/2004

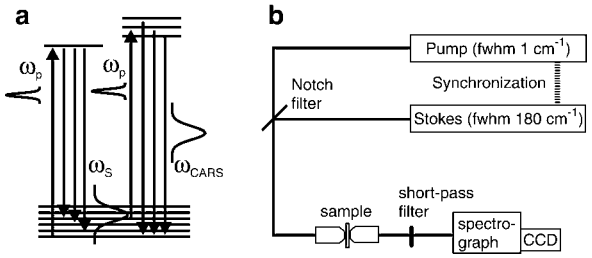

Figure 1. (a) Energy level diagram of the multiplex CARS process. (b) Scheme of the experimental setup.

(L) in a solvent (S) is well described by

$$I_{CARS} \propto |N_S\chi^{(3)}_{NR} + N_L\chi^{(3)}_R|^2 = (N_S\chi^{(3)}_{NR})^2 + 2N_SN_L\chi^{(3)}_{NR}[Re(\chi^{(3)}_R)] + N_L{}^2|\chi^{(3)}_R|^2 \quad (1)$$

where N denotes the number of molecules and $\chi^{(3)}_{NR}$ and $\chi^{(3)}_R = \sum_j A_j/[\Omega_j - (\omega_p - \omega_S) + i\Gamma_j]$ represent the (real) nonresonant and (imaginary) resonant components of the third-order nonlinear susceptibility, respectively. The vibrational resonances are described by their resonance frequencies Ω_j, amplitudes A_j, and line widths: full-width at half-maximum, fwhm $= 2\Gamma_j$. In eq 1, it is assumed that the solvent has no vibrationally resonant contribution and that the nonresonant contribution of the solute can be neglected. Thus, the total CARS signal is composed of three terms: a squared background signal, a cross-term, and the squared resonant signal. In background-free CARS schemes, the goal is to detect only the latter term by suppressing the nonresonant background. In this case, the signal intensity falls off with the square of the solute concentration. In multiplex CARS, on the other hand, the total signal is detected, where the resonant contribution is dominated by the heterodyne cross term ($\chi^{(3)}_{NR}\chi^{(3)}_R$) that falls off linearly with the solute concentration. There is a unique correspondence between CARS and spontaneous Raman spectra when both are taken under parallel polarization conditions; hence, the resonant contributions are easily extracted from the total signal.

The experimental setup is based on a collinear phase-matching configuration of pump and Stokes pulses, which are synchronized in time and focused by a high numerical aperture microscope objective. The setup has been described in detail elsewhere.[3] The pump laser operates in picosecond mode, with pulses of 10 ps (bandwidth ~1 cm^{-1} fwhm), centered around 710 nm. The Stokes pulses have a duration of 80 fs, corresponding to a bandwidth of ~180 cm^{-1} fwhm and can be tuned from 700 to 950 nm, which covers 300−3500 cm^{-1}; almost the full range of molecular vibrations. Typically, the average powers of the pump and Stokes lasers are 200 and 15−25 mW, respectively. We omitted the grating pair that was previously used to stretch the Stokes pulse in time. The spectral resolution of ~5 cm^{-1} is determined by the spectrograph. An outline of the multiplex CARS setup is schematically shown in Figure 1b. Raman spectra were measured with a Raman microscope (Renishaw RM1000, spectral resolution: ~5 cm^{-1}) with a 6 mW HeNe laser.

All lipids were obtained from Avanti Polar lipids. For the gel-phase lipids, 1,2-dipalmitoyl-sn-glycero-3-phosphocholine (DPPC, 16:0) and 1,2-dipalmitoyl-D62-*sn*-glycero-3-phosphocholine (*d62*-DPPC, 16:0), supported planar bilayers (SPB) were prepared on glass coverslips using the Langmuir−Blodgett technique at a surface pressure of 32 mN m^{-1}. The quality of the bilayer could be assessed from the transfer ratio, which was always close to one. With the liquid-phase lipid, 1,2-dioleoyl-*sn*-glycero-3-phosphocholine (DOPC; 18:1, 9-cis), SPBs were formed using vesicle fusion.[15] Alternatively, for asymmetric bilayers, DOPC vesicles were fused to a glass substrate that had previously been covered with a *d62*-DPPC monolayer using the Langmuir−Blodgett technique. After rinsing with Millipore water, a single bilayer remained on the glass surface. For all lipids, these procedures were checked by adding 1 mol % 1,1′-dioctadecyl-3,3,3′,3′-tetramethylindocarbocyanine perchlorate (diIC$_{18,}$ Molecular Probes) to the lipids. Using a fluorescence microscope with a 100× objective, the SPB appeared homogeneous.

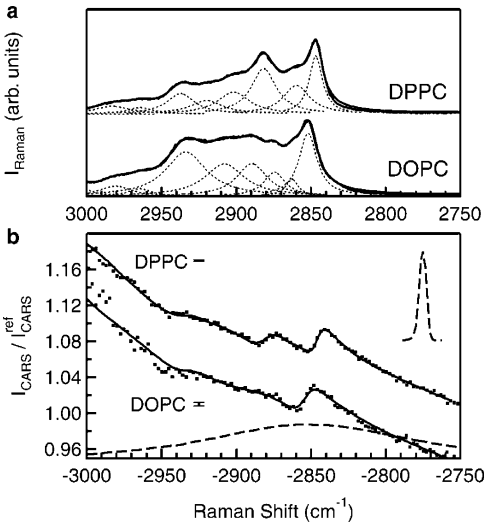

Figure 2. (a) Spontaneous Raman scattering spectra of DPPC and DOPC fitted with a sum of Lorentzian line shapes. The individual Lorentz contributions are also shown. (b) Multiplex CARS spectra of DPPC (vertically offset by 0.08) and DOPC lipid bilayers on the glass-water interface divided by the glass spectrum. Exposure times are 2.5 and 0.5 s, respectively. Error bars indicate the shot-noise standard deviation. Data were fitted using eq 2, constraining the peak positions and widths to the values obtained from the Raman fit. The dashed lines indicate the multiplex CARS signal of glass (bottom) and the spectral resolution of the setup (top right).

The lipid bilayers at the glass-water interface were measured by making a *z* scan through the membrane. All multiplex CARS spectra, I_{CARS}, were divided by a reference spectrum, I^{ref}_{CARS}, measured in the coverglass. I_{CARS}/I^{ref}_{CARS} of DPPC and DOPC bilayers measured in the C−H stretch region at the glass−water interface are shown in Figure 2b together with the corresponding Raman spectra of bulk, anhydrous lipids on CaF_2 [Figure 2a]. For DPPC, a gel-phase lipid, the most prominent features are the two sharp peaks at 2847 and 2882 cm^{-1}, assigned to $\nu_s(CH_2)$ and $\nu_a(CH_2)$ the symmetric and asymmetric methylene stretch vibrations, respectively. The broad peak around 2840 is ascribed to a Fermi resonance $\nu_s(CH_3)_{FR}$.[16] In a liquid-crystalline phase, the Raman spectrum shows some marked changes as can be seen for DOPC: most notably, $\nu_a(CH_2)$ loses intensity with respect to $\nu_s(CH_2)$ which in turn shifts to higher wavenumbers.

The qualitative differences between gel and liquid crystalline phase of the bulk lipids are directly reflected in the multiplex CARS spectra of the bilayers. As shown in Figure 2(b): in the DPPC spectrum $\nu_s(CH_2)$, $\nu_a(CH_2)$ and $\nu_s(CH_3)_{FR}$ can be clearly discerned, whereas in the DOPC spectrum, only $\nu_s(CH_3)_{FR}$ and $\nu_s(CH_2)$ are visible. The latter is also shifted to higher wavenumbers in accordance with the Raman spectrum.

To more accurately retrieve the spectral parameters, least-squares fitting of the multiplex CARS data was performed, using

a modified form of eq 1

$$\frac{I_{\mathrm{CARS}}}{I_{\mathrm{CARS}}^{\mathrm{ref}}}(\omega_{\mathrm{p}}-\omega_{\mathrm{s}})=\frac{1}{|\chi_{\mathrm{NR}}^{\mathrm{glass}}|^2}\left|\chi_{\mathrm{NR}}+n_{\mathrm{w}}\chi_{\mathrm{R}}^{\mathrm{water}}(\omega_{\mathrm{p}}-\omega_{\mathrm{s}})+\sum_j\frac{A_j}{\Omega_j-(\omega_{\mathrm{p}}-\omega_{\mathrm{S}})+i\Gamma_j}\right|^2 \quad (2)$$

where $\chi_{\mathrm{NR}}/\chi_{\mathrm{NR}}^{\mathrm{glass}}$ is a frequency independent parameter that describes the total nonresonant background in the focal volume relative to the glass nonresonant background and n_{w} is a parameter that mixes in a certain amount of the resonant water spectrum that was recorded separately. The amplitudes (A_j), line widths (Γ_j), and spectral positions (Ω_j) of lipid vibrational resonances correspond to the parameters that were used to fit the spontaneous Raman spectra with a sum of normalized Lorentzians. Although water has only a weak resonant Raman scattering cross section at these vibrational frequencies, inclusion of the resonant water contribution in eq 2 is essential for reliable fits of the multiplex CARS data at this level of sensitivity. For the fit of the multiplex CARS spectra, the peak positions and widths were constrained to the values obtained from the Raman fit, whereas all other parameters were optimized. As shown in Figure 2b, the multiplex CARS spectra of both DPPC and DOPC bilayers can be fitted very well with eq 2.

The region around 3000 cm^{-1} of the Raman spectrum consists of a large number of overlapping peaks, containing both fundamental CH-stretch vibrations and Fermi resonance bands. The relative intensities of these peaks change notably with changes in hydration state, packing, and conformational order. To utilize this spectral sensitivity toward the lipid environment, several spectral parameters have been used in the literature that empirically describe the order of the lipid bilayer.[16−18] Here, the peak height ratio $R = I[\nu_{\mathrm{a}}(\mathrm{CH_2})]/I[\nu_{\mathrm{s}}(\mathrm{CH_2})]$ has been used as a marker for chain packing and conformational disorder, where higher values indicate a higher ordering of the chains. This order parameter was determined for the CARS spectra of DPPC and DOPC planar supported bilayers (PSB) and compared to the values obtained from CARS spectra of lipid multilamellar vesicles (MLV). The CARS spectra were analyzed as follows: the spectra were first fit as described above, after which the corresponding Raman spectrum was calculated from the fit parameters. R could then be determined from the calculated Raman spectrum.

In MLVs, R is found to be higher for the gel phase lipid DPPC than for the liquid-phase lipid DOPC, i.e., $R = 0.79 \pm 0.04$ and 0.69 ± 0.03 respectively (data not shown). This confirms the well-known higher ordering of the lipids in the gel phase. For the PSBs, R again is higher for DPPC ($R = 0.99 \pm 0.09$) than for DOPC (0.74 ± 0.08). Interestingly, DPPC shows a significant difference between MLV and PSB system, whereas for DOPC, the order parameter is the same for both lipid systems within experimental error. This can be understood by noting that in the gel phase when the acyl chains are extended, R is sensitive *only* to lateral packing order.[17] It can be envisaged that on a glass support, the lipid acyl chains are more orderly packed, than in a MLV. In contrast, when the lipids are in a liquid phase, R is additionally sensitive to conformational ordering of the chains. The latter is not expected to differ much between MLV and PSB.[19]

As shown above, a distinction between different thermodynamic phases of a bilayer can be made solely based on the C−H stretch vibrations of the lipids, using the Raman spectrum for guidance. Specific labeling can be accomplished with deuterated lipids that show C−D stretch vibrations in a distinct window of the Raman spectrum. With deuterated lipids in one of the leaflets, spectra can be recorded from a single leaflet despite the insufficient axial resolution. We studied a *d62*-DPPC planar supported bilayer together with a asymmetric bilayer system containing a *d62*-DPPC monolayer proximate to the glass and a distal monolayer of DOPC. Multiplex CARS spectra of these samples are shown in Figure 3, together with the corresponding Raman spectra. Note that the measured signal strength (i.e., the total vibrationally resonant contribution divided by the nonresonant contribution) provides an absolute measure for the number of vibrationally resonant molecules within the focal volume and is independent of actual laser powers. Using a line shape analysis, relating the CARS peak intensity to the fit parameters as $A_j/(\pi\Gamma_j\chi_{\mathrm{NR}})$, we obtain a $\nu_{\mathrm{s}}(\mathrm{CD_2})$ signal of the monolayer ($1.1 \pm 0.3 \times 10^{-3}$) which is half that of the bilayer ($2.0 \pm 0.4 \times 10^{-3}$) within experimental error.

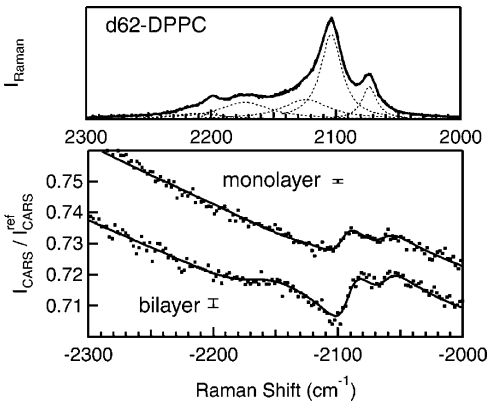

Figure 3. (Top) Spontaneous Raman scattering spectra of *d62*-DPPC fitted with a sum of Lorentzian line shapes. (Bottom) Corresponding multiplex CARS spectra of *d62*-DPPC bilayer and monolayer on the glass-water interface divided by the glass spectrum. Exposure time: 0.64 s. Error bars indicate the shot-noise standard deviation. Data were fitted using eq 2, using three peaks to describe the data.

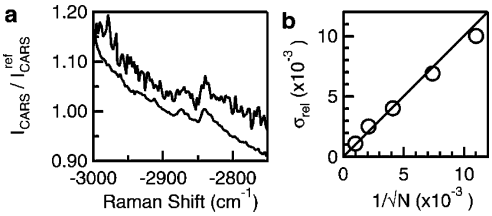

Figure 4. (a) Demonstration of the shot-noise limited multiplex CARS sensitivity with a DPPC bilayer on the glass-water interface. The top spectrum (vertically offset by 0.02) was recorded in 20 ms, whereas the bottom spectrum was measured with an exposure time of 1.28 s. (b) The SNR is governed only by Poisson statistics.

The local lipid concentration of a planar bilayer in the center of the microscope focus can be estimated to be approximately 5 mM (9×10^{-5} lipid:water molar ratio), assuming a lipid area of 50 Å^2 and an ellipsoid focal volume with a radius of 0.3 μm and height of 1.0 μm.[4] As shown in Figure 3a for a DPPC bilayer, at such low concentrations, the main features of a multiplex CARS spectrum can readily be detected with a SNR of 4 for the -2850 cm^{-1} feature at an exposure time of 20 ms. Better quality spectra, revealing more spectral details at a SNR of 12.4 can be achieved by longer integration as demonstrated for the same sample recorded with an exposure time of 1.28 s. At this increased SNR level, even the broad and relatively weak $\nu_{\mathrm{s}}(\mathrm{CH_3})_{\mathrm{FR}}$ resonance around -2940 cm^{-1} becomes clearly identifiable. As shown in Figure 4b, the relative standard

deviation of the noise (σ_{rel}) equals $1/\sqrt{N}$, where N is the number of detected photons. Therefore, the SNR is limited only by shot-noise.

The results presented here demonstrate the value of multiplex CARS for high sensitivity vibrational imaging. The shot-noise limited sensitivity is not reached by rejecting the nonresonant background but by collection of the complete CARS signal over a range of frequencies. Therefore, the signal drops linearly instead of quadratically with the solute concentration, while retaining the spectral information that allows us to discern different molecules in different phases. In combination with the possibility to "label" a sample with deuterated analogues, this technique shows great potential as an imaging technique in life and material sciences.

Acknowledgment. The authors thank M. Bonn for a critical reading of the manuscript. This research was financially supported, in part, by the Stichting voor Fundamenteel Onderzoek der Materie (FOM) and Aard-en Levenswetenschappen (ALW), The Netherlands under Grant Nos. 805.47.040 and 94RG02.

References and Notes

(1) Duncan, M. D.; Reintjes, J.; Manuccia, T. J. *Opt. Lett.* **1982**, *7*, 350.

(2) Zumbusch, A.; Holtom, G. R.; Xie, X. S. *Phys. Rev. Lett.* **1999**, *82*, 4142.

(3) Müller, M.; Schins, J. M. *J. Phys. Chem. B* **2002**, *106*, 3715.

(4) Wurpel, G. W. H.; Schins, J. M.; Müller, M. *Opt. Lett.* **2002**, *27*, 1093.

(5) Potma, E. O.; Xie, X. S. *J. Raman Spectrosc.* **2003**, *34*, 642.

(6) Edidin, M. *Annu. Rev. Biophys. Biomol. Struct.* **2003**, *32*, 257.

(7) Akhmanov, S. A.; Bunkin, A. F.; Ivanov, S. G.; Koroteev, N. I. *Sov. Phys. JETP* **1978**, *47*, 667.

(8) Oudar, J.-L.; Smith, R. W.; Shen, Y. R. *Appl. Phys. Lett.* **1979**, *34*, 758.

(9) Cheng, J. X.; Volkmer, A.; Book, L. D.; Xie, X. S. *J. Phys. Chem. B* **2001**, *105*, 1277.

(10) Volkmer, A.; Book, L. D.; Xie, X. S. *Appl. Phys. Lett.* **2002**, *80*, 1505.

(11) Oron, D.; Dudovich, N.; Silberberg, Y. *Phys. Rev. Lett.* **2003**, *90*, 213902.

(12) Ishibashi, T. A.; Onishi, H. *Appl. Phys. Lett.* **2002**, *81*, 1338.

(13) Richter, L. J.; Petralli-Mallow, T. P.; Stephenson, J. C. *Opt. Lett.* **1998**, *23*, 1594.

(14) Oron, D.; Dudovich, N.; Silberberg, Y. *Phys. Rev. Lett.* **2002**, *89*, 273001.

(15) Rinia, H. A.; Snel, M. M. E.; van der Eerden, J.; de Kruijff, B. *FEBS Lett.* **2001**, *501*, 92.

(16) Levin, I. W. Vibrational spectroscopy of membrane assemblies. In *Advances in infrared and Raman spectroscopy*; Clark, R. J. H., Hester, R. E., Eds.; Wiley: London, 1984; Vol. 11, p 1.

(17) Snyder, R. G.; Hsu, S. L.; Krimm, S. *Spectrochim. Acta A* **1978**, *34*, 395.

(18) Orendorff, C. J.; Ducey Jr., M. W.; Pemberton, J. E. *J. Phys. Chem. A* **2002**, *106*, 6991.

(19) Linseisen, F. M.; Hetzer, M.; Brumm, T.; Bayerl, T. M. *Biophys. J.* **1997**, *72*, 1659.